Precambrian Research 259 (2015) 278–289

Contents lists available at ScienceDirect

Precambrian Research

journal homepage: www.elsevier.com/locate/precamres

Is the rate of supercontinent assembly changing with time?

Kent Condie[a,*], Sergei A. Pisarevsky[b,c], Jun Korenaga[d], Steve Gardoll[e]

[a] Department of Earth & Environmental Science, New Mexico Tech, Socorro, NM 87801, USA
[b] Australian Research Council Centre of Excellence for Core to Crust Fluid Systems (CCFS), School of Earth and Environment, University of Western Australia, Crawley, WA 6009, Australia
[c] Institute for Geoscience Research (TIGeR), Department of Applied Geology, Curtin University, GPO Box U1987, Perth, WA 6845, Australia
[d] Department of Geology and Geophysics, Yale University, PO Box 208109, New Haven, CT 06520-8109, USA
[e] Department of Applied Geology, Curtin University, GPO Box U1987, Perth, WA 6845, Australia

ARTICLE INFO

Article history:
Received 17 February 2014
Received in revised form 3 June 2014
Accepted 26 July 2014
Available online 4 August 2014

Keywords:
Supercontinent cycle
Plate tectonics
Collisional orogens
Passive margins
Plate speeds

ABSTRACT

To address the question of secular changes in the speed of the supercontinent cycle, we use two major databases for the last 2.5 Gyr: the timing and locations of collisional and accretionary orogens, and average plate velocities as deduced from paleomagnetic and paleogeographic data. Peaks in craton collision occur at 1850 and 600 Ma with smaller peaks at 1100 and 350 Ma. Distinct minima occur at 1700–1200, 900–700, and 300–200 Ma. There is no simple relationship in craton collision frequency or average plate velocity between supercontinent assemblies and breakups. Assembly of Nuna at 1700–1500 Ma correlates with very low collision rates, whereas assemblies of Rodinia and Gondwana at 1000–850 and 650–350 Ma, respectively correspond to moderate to high rates. Very low collision rates occur at times of supercontinent breakup at 2200–2100, 1300–1100, 800–650, and 150–0 Ma. A peak in plate velocity at 450–350 Ma correlates with early stages of growth of Pangea and another at 1100 Ma with initial stages of Rodinia assembly following breakup of Nuna. A major drop in craton numbers after 1850 Ma corresponds with the collision and suturing of numerous Archean blocks.

Orogens and passive margins show the same two cycles of ocean basin closing: an early cycle from Neoarchean to 1900 Ma and a later cycle, which corresponds to the supercontinent cycle, from 1900 Ma to the present. The cause of these cycles is not understood, but may be related to increasing plate speeds during supercontinent assembly and whether or not long-lived accretionary orogens accompany supercontinent assembly. LIP (large igneous province) age peaks at 2200, 2100, 1380 (and 1450?), 800, 300, 200 and 100 Ma correlate with supercontinent breakup and minima at 2600, 1700–1500, 1100–900, and 600–400 Ma with supercontinent assembly. Other major LIP age peaks do not correlate with the supercontinent cycle. A thermochemical instability model for mantle plume generation can explain all major LIP events by one process and implies that LIP events that correspond to the supercontinent cycle are independent of this cycle.

The period of the supercontinent cycle is highly variable, ranging from 500 to 1000 Myr if the late Archean supercratons are included. Nuna has a duration of about 300 Myr (1500–1200 Ma), Rodinia 100 Myr (850–750 Ma), and Gondwana–Pangea 200 Myr (350–150 Ma). Breakup durations are short, generally 100–200 Myr. The history of angular plate velocities, craton collision frequency, passive margin histories, and periodicity of the supercontinent cycle all suggest a gradual speed up of plate tectonics with time.

1. Introduction

The supercontinent cycle as proposed by Worsley et al. (1984, 1985) and now widely accepted is important in understanding the tectonic history of continents, and it also provides a powerful constraint on the climatic and biologic evolution of Earth. The overall characteristics and history of the development of the supercontinent cycle is reviewed in detail by Nance and Murphy (2013) and Nance et al. (2014) and will not be repeated. Lowman and Jarvis (1995) and Gurnis (1988) suggested that continental blocks tend to be drawn to mantle downwellings where they may collide to form supercontinents. Because of their thickness and enrichment in U, Th and K, supercontinents should act as thermal insulators to mantle heat (Anderson, 1982; Gurnis, 1988), but

* Corresponding author.
E-mail address: kcondie@nmt.edu (K. Condie).

http://dx.doi.org/10.1016/j.precamres.2014.07.015
0301-9268/

consideration based on the thermal budget of the Earth indicates that the actual effect of insulation is likely to be weak, probably no more than an increase of 20 °C in mantle temperature (Korenaga, 2007). Perhaps more important is the global organization of mantle flow pattern caused by the presence of a supercontinent (e.g., Storey, 1995). Recent numerical simulation studies suggest that after a supercontinent is assembled over a downwelling in one hemisphere, circum-supercontinent subduction induces a new major upwelling beneath the supercontinent transforming a degree-1 planform in the mantle into a degree-2 planform with two antipodal downwellings (Zhong et al., 2007; Zhang et al., 2009).

We still have many questions regarding the supercontinent cycle, such as when it began, has continental crust grown in volume with time, and has the period of the cycle been constant or has it changed with time. The timescale of assembly and dispersal of supercontinents is still not well constrained, with estimates of cycle length ranging from 250 Myr to 1000 Myr (Phillips and Bunge, 2007; Zhang et al., 2009; Yoshida and Santosh, 2011). Some investigators have suggested that the supercontinent cycle has speeded up with time (Hoffman, 1997; Condie, 2002), but testing such an idea is not easy because it involves how a supercontinent is defined, and whether or not large blocks of one supercontinent survive during breakup to become incorporated in later supercontinents. The secular change in the supercontinent cycle is, however, an important problem in the evolution of plate tectonics. It is commonly assumed that a hotter mantle in the past resulted in faster plate motions (e.g., Schubert et al., 1980; Davies, 2009), which could be reflected in the formation history of supercontinents.

In this study, we address the question of whether the supercontinent cycle is speeding up, slowing down, or remaining constant with time. Our primary datasets are angular plate speeds as deduced from published paleogeographic reconstructions, paleomagnetic studies, and the frequency of collisional and accretionary orogeny as estimated from extensive geologic and geochronologic data. We also address the question of ocean basin closing and how it may have changed with time, and compare results to the cycles and durations of sedimentation in passive margins. From these data, we discuss the lifetimes of supercontinents and possible relationship to mantle plume activity as deduced from LIP (large igneous province) events through time. We conclude that average plate speed and the collisional frequency of cratons are probably increasing with time, and that the supercontinent cycle, which began about 1750 Ma, is also speeding up with time.

2. Methods

2.1. Characteristics of orogens

In previous papers we have discussed the compilation of orogen characteristics and uncertainties, and this will not be repeated (Condie, 2013, 2014). One of the main sources of uncertainty in counting orogens is that of what to count as a single orogen. Collisional orogens of short strike length could be part of a longer orogen, now displaced by later supercontinent breakup. Hence, most of the orogens listed in Appendix 1 are really "orogen segments". In some cases an orogen segment may represent a complete orogen, whereas in others, it may represent only part of an orogen that was originally much more extensive. This problem is especially difficult when orogens wrap around cratons with "swirly" patterns as they do in Gondwana. In these cases, no more than one orogen segment is counted along a given craton margin. In very long orogens, such as the Great Proterozoic Accretionary Orogen (Condie, 2013) (Fig. 1, number 35), some portions of the orogen that have been well studied are designated as segments.

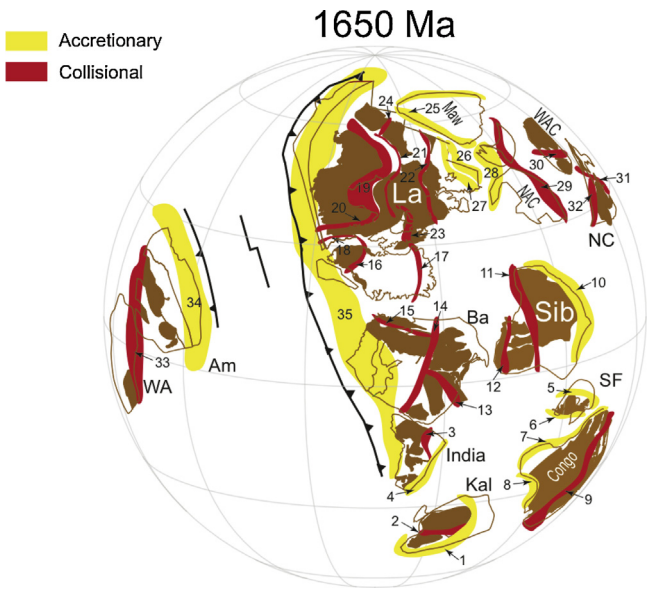

Fig. 1. Paleogeographic reconstruction of cratons during the late stages of Nuna assembly at 1650 Ma (from Pisarevsky et al., 2014a). Orogens from Appendix 1 (Pts 1 and 2). *Key*: cratons: Kal, Kalahari; SF, São Francisco; Sib, Siberia; La, Laurentia; Maw, Mawson; NAC, North Australian craton; WAC, West Australian craton; NC, North China; Am, Amazonia; WA, West Africa. orogens: 1, Magondi-Kheis (2.04–1.96 Ga); 2, Limpopo (2.06–1.97 Ga); 3, Aravalli (1.87–1.85 Ga); 4, Lesser Himalaya (1.88–1.78 Ga); 5, Borborema (2.35–2.30 Ga); 6, Mineiro (2.45–2.36 Ga); 7, West Congo (2.1–2.0 Ga); 8, Luizian (2.1–2.0 Ga); 9, Ubendian (1.88–1.85 Ga); 10, Angara (1.9–1.85 Ga); 11, Akitkan (1.9–1.87 Ga); 12, Sutam (1.9–1.85 Ga); 13, Volga-Don (2.05–2.0 Ga); 14, Volhyn-Central Russian (1.80–1.78 Ga); 15, Lapland Granulite Belt (1.92–1.87 Ga); 16, Nagssugtoqidian (1.87–1.84 Ga); 17, Inglefield (1.95–1.92 Ga); 18, Torngat (1.87–1.84 Ga); 19, Trans-Hudson (1.85–1.80 Ga); New Quebec (1.87–1.82 Ga); 21, Arrowsmith (2.4–2.3 Ga); 22, Thelon (1.96–1.91 Ga); Foxe (1.87–1.85 Ga); 24, Big Sky (1.8–1.7 Ga); 25, Nimrod-Ross (1.84–1.73 Ga); Racklan-Forward (1.64–1.60 Ga); 27, Wopmay (1.9–1.84 Ga); 28, Olarian (1.58–1.54 Ga); 29, Kimban-Yapungku (1.83–1.70 Ga); 30, Glenburgh (1.97–1.94 Ga); 31, Trans-North China (1.89–1.85 Ga); 32, Khondalite (1.95 Ga); 33, Birimian-Transamazonian (2.1–2.05 Ga); 34, Amazonia (2030–1000 Ma); 35, Great Proterozoic Accretionary Orogen (1900–1100 Ma).

In this study, a major distinction between collisional and accretionary orogens is made based on how they end: collisional orogens end with continent-continent collisions (Appendix 1, Pt 1). Accretionary orogens, on the other hand, do not always end with a continent-continent collision as did India and Tibet. Rather they may end by subduction of an ocean ridge, regional plate reorganizations, a change in plate boundary from convergent to transform (such as the San Andreas fault), or collision of a major terrane or continental island arc (Condie, 2007; Cawood et al., 2009; Moores et al., 2013). A major terrane collision may shut down activity in one segment of an orogen and initiate activity along strike in another segment. Very often collisional and accretionary orogens can develop simultaneously with supercontinent assembly. In the last 300 Myr, for instance, peripheral accretionary orogens have developed simultaneously with collisional orogens responsible for aggregation of Pangea (Cawood and Buchan, 2007; Cawood et al., 2009).

2.2. Plate speeds

Paleomagnetic data provide a quantitative tool for paleogeographic reconstructions. However, the number of high-quality paleomagnetic results is limited, especially for the Early-Middle Paleozoic and Precambrian (e.g. Van der Voo, 1993; McElhinny and McFadden, 2000; McElhinny et al., 2003; Pisarevsky et al., 2003, 2014a,b; Li et al., 2008). Consequently the most complete and reliable published global paleogeographic reconstructions for

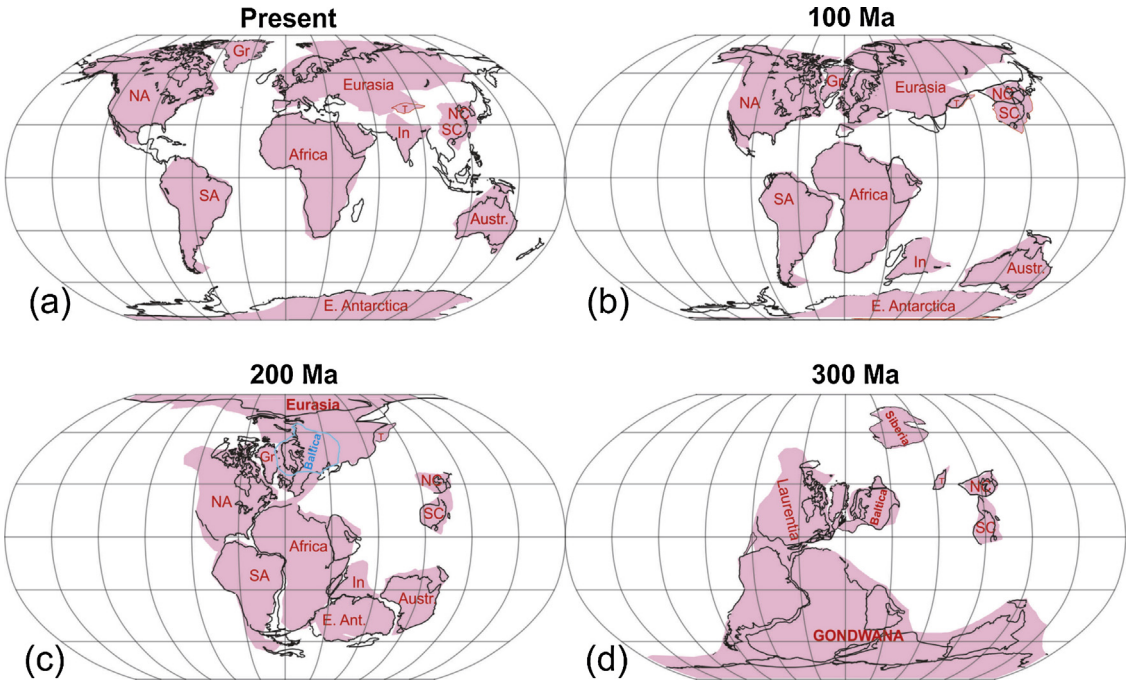

Fig. 2. Late Paleozoic and Mesozoic paleogeographic reconstructions of major continents. NA = North America, SA = South America, Gr = Greenland, NC = North China, SC = South China, In = India. Euler rotation parameters are given in Appendix 1 (Pt 3). The estimated area of each rigid continent is shaded in pink. These areas were used for the angular velocity calculations.

the last 2 Gyr are constrained by both geological and paleomagnetic data including the following: (i) all major continental block positions are shown in the reconstructions; (ii) evolving block positions are known in time slices or animations; (iii) reconstructions are made with computer software using spherical geometry; and (iv) each reconstruction is made with Euler rotation parameters.

Although we analyze data over the last 2.5 Gyr, neither paleomagnetic data nor paleogeographic reconstructions are equally reliable at all ages. For example, only two Proterozoic – Early Cambrian time intervals are covered by published global paleogeographic models: (i) 1100–530 Ma with two alternative subsets at 615–550 Ma (Li et al., 2008) and (ii) 1770 –1270 Ma (Pisarevsky et al., 2014a,b). Pre-1770 Ma reconstructions are rare, controversial and sometimes sketchy (e.g. Pesonen et al., 2003; Ernst and Bleeker, 2010), which is related to a scarcity of reliable paleomagnetic data. For instance, compiled only 17 well dated and reliable paleopoles from 6 proto-cratons (Superior, Kaapvaal, Zimbabwe, Kola-Karelia, Dharwar and Yilgarn) for the 700 Myr time interval between 2.5 and 1.8 Ga. Moreover, only the Superior craton has several poles for different time slices. The time interval between 1270 and 970 Myr is also poorly represented by paleomagnetic data, and paleopositions of most continents are controversial, with only Laurentia adequately constrained by paleomagnetic data.

For supercontinent reconstructions we use various Phanerozoic paleogeographic models (Lawver et al., 2002; Torsvik et al., 2001; Li and Powell, 2001; McElhinny et al., 2003; Collins and Pisarevsky, 2005), and for the Neoproterozoic we generally follow Li et al. (2008) with some modifications for the 900–800 Ma time interval (Pradhan et al., 2008; Wingate et al., 2010). As Li et al. (2008) consider two sets of global reconstructions between 615 and 550 Ma, we use the "low-latitude" model favored by recent publications (e.g. Levashova et al., 2013). For the 1770–1270 Ma time interval we follow the paleogeographic model of Pisarevsky et al. (2014a,b). As the sizes of continents vary significantly, we calculate the mean angular velocity for each 100 Myr bin by normalizing to continental area as follows:

$$\text{mean angular velocity of } n \text{ continents} = \frac{\sum_{i=0}^{n} v_i s_i}{\sum_{i=0}^{n} s_i}$$

where s_i is the area of the ith continent (km^2) and v_i is the angular velocity of this continent (degrees/100 Myr).

We studied only the movement of continental plates, because the data from oceanic plates are not available for most of the time period of interest (≤2.7 Ga). Second, we analyze only the movements of large continents (Fig. 2), because data for the rotations of small blocks in accretionary orogens are rare and not well constrained (e.g. Cawood et al., 2011). With two exceptions (2500–1770 Ma and 1270–1000 Ma) high quality paleomagnetic data are not available for the reconstructions. Instead we analyze a series of global paleogeographic reconstructions in 100 Myr time intervals and calculate Euler angles between positions of each analyzed continent on later reconstructions. For example, we estimate the average angular velocity of Africa in the last 100 Myr as the angle of rotation of Africa 100 Ma (Fig. 2b) compared to its present position (Fig. 2a). We also considered breakup and suturing of cratons at different times. For example in the last 200 Myr, Siberia and Baltica were parts of a single continent (Fig. 2a–c), but before that they moved separately (Fig. 2d). Consequently we calculate the average angular velocity of Baltica and Siberia separately before 200 Ma, but after this time we consider them both as part of the single continent Eurasia. On the other hand, before 200 Ma we calculate velocities for Gondwana as a single continent (Fig. 2d), whereas afterwards we calculate velocities of single segments of Gondwana (Africa, South America etc.) separately.

3. Results

3.1. Frequency of craton collisions

As shown in Fig. 3, there is quite a scatter in frequency of continental plate collisions ranging from about one to 20 per 100 Myr, with an average of six. Uncertainty of the data is about

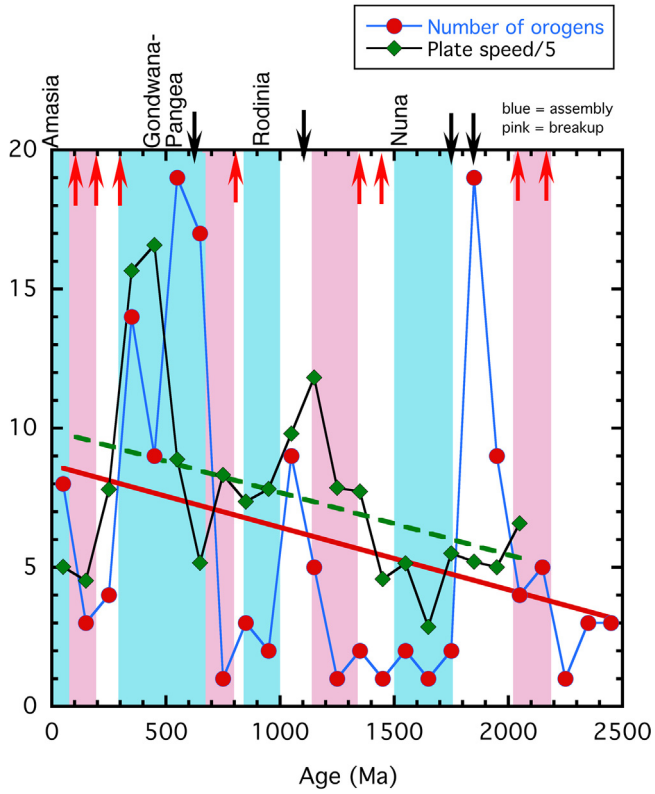

Fig. 3. Secular changes in craton collision frequency and average area-weighted plate speed (deg/100 Myr). Collision frequency between cratons is expressed as number of orogen segments per 100-Myr bin moving in 100 Myr increments (data from Appendix 1, Pt 2). Lines are linear regression analysis: $n = 8.68–0.00224a$, $r = 0.287$; $s = 9.927–0.00223a$, $r = 0.393$ (n, number of orogens; s, plate speed divided by five; a, age). Also shown are supercontinent assembly (blue stripes) and breakup (pink stripes) times. Major LIP (large igneous provinces) events: red arrows correspond to LIPs associated with supercontinent breakup black arrows correspond to other LIPs (unpub. LIP database, K. C. Condie, 2014).

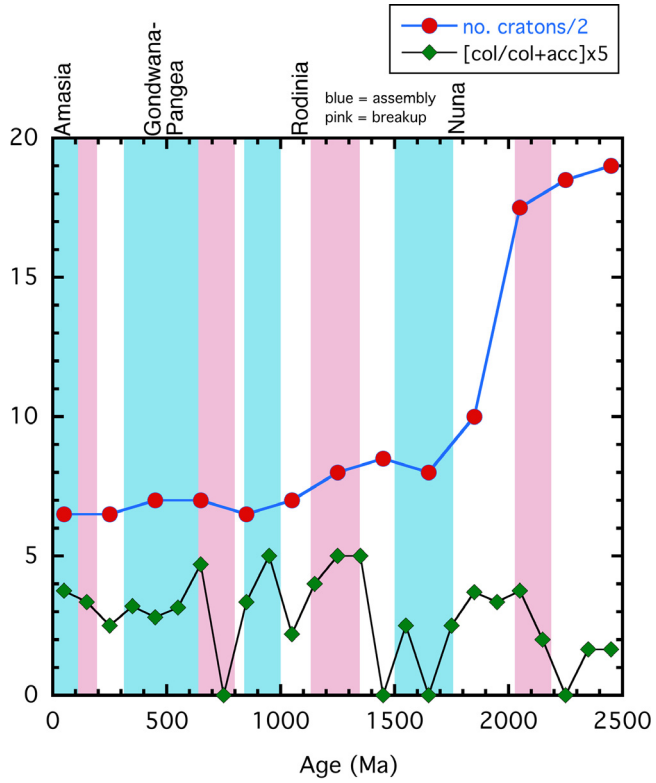

Fig. 4. Secular change in number of cratons with time; each red dot is the number of cratons/2. Also shown is the ratio of collisional to collisional + accretionary orogens (col/[col + acc]) with time. Other information given in caption of Fig. 3.

±2 orogens per 100-Myr time window. High collision rates are observed at 1850 and 600 Ma with smaller peaks at about 1100 and 350 Ma. Distinct minima occur at 1700–1200, 900–700, and 300–200 Ma, and a possible minimum around 450 Ma. Collision rates also increase during the beginnings of a possible new supercontinent Amasia in the last 100 Myr. As expected, relatively low collision rates occur at times of supercontinent breakup (2200–2100, 1300–1200, 800–700, and 300–100 Ma). The 1850 Ma peak is unique in that it correlates with numerous collisions between small Archean cratons that were dispersed during breakup of late Archean supercratons at 2200–2100 Ma. In contrast to low collisional rates during final stages of Nuna assembly at 1700–1500 Ma, moderate to high collision rates are characteristic for the early stages of supercontinent assemblies (e.g. Rodinia at 1100–1000 Ma; Gondwana at 600–500 Ma).

Linear regression analysis of the data shows that despite the large variation in number of orogens with time, the frequency of collisional orogeny increases with time (Fig. 3). In the late Archean, the frequency is around 3 collisions/100 Myr, increasing to an average of 8–9 collisions/100 Myr in the last 200 Myr.

Another variable of interest is the ratio of collisional (col) to accretionary (acc) orogens with time. To avoid the problem that many accretionary orogens evolve into collisional orogens, we have used the termination time of orogens to classify them as accretionary or collisional; at least one margin of collisional orogens went through an accretionary stage before collision. Expressed as the col/[col + acc] ratio, the fraction of orogens that are collisional is quite variable ranging from zero to one, and there is no clear relationship between assemblies and breakups of supercontinents (Fig. 4). During assembly, Nuna has a low col/[col + acc] ratio reflecting the development of Great Proterozoic Accretionary Orogen (Fig. 1) and related accretionary orogens. The low at 750 Ma correlates with Rodinia breakup, although this is based on only one orogen in the 800–700 Ma time window. Breakup times of other supercontinents do not show minima in the col/[col + acc] ratio.

3.2. Number of dispersed cratons with time

There are several sources of uncertainty in estimating the number of cratons during supercontinent breakup and dispersal. Most important is how to define a craton, and what is the minimum craton size that can be confidently identified in the geologic record. If we define a craton as a continental plate with a size greater than or equal to the size of the North China craton (Fig. 1), the number of cratons decreases from ≥20 before 1900 Ma to <20 after this time (Fig. 4). This large drop in craton numbers correlates with the collision and suturing of numerous Archean blocks at this time. From 1900 Ma onwards there is a steady drop from 20 to 13–17 cratons per 200 Myr window. If real, this trend indicates that each time a supercontinent fragmented in the last 1800 Myr, it resulted in fewer pieces. However, there are no striking jumps in craton numbers like that at 1900 Ma during later supercontinent assemblies. These pieces may also be progressively larger if the recycling rate of continental crust into the mantle is not increasing over this same time interval. This long-term trend in the number of cratons implies that cratons tend to stick together once they are juxtaposed. Such behavior is

possible if the strength of sutures is greater than typical convective stresses.

3.3. Angular plate velocities

Angular plate velocities as weighted by craton area show considerable variation, ranging from about 20 to 80 deg/100 Myr with an average of 38 deg/100 Myr (Fig. 3). Velocity peaks occurs at 450–350 Ma and near 1100 Ma with velocities of 60–80 deg/100 Myr. The former peak correlates with early stages of Pangea assembly and is due primarily to the rapid motion of Gondwana; this peak is also recognized by Phillips et al. (2009). However, unlike Pangea and Rodinia, the early stages of Gondwana assembly at 650–550 Ma correspond to a minimum in plate velocities. The 1100-Ma peak may correspond with the early stages in Rodinia assembly, however, the timing is not well known from paleomagnetic data. Average plate speeds are remarkably low during the assembly of Nuna at 1700–1500 Ma (15–20 deg/100 Myr), and the low at 150 Ma corresponds to the onset of breakup of Gondwana–Pangea at 200–180 Ma and the possible beginnings of assembly of a new supercontinent Amasia. Thus, it would appear that there is no simple relationship in average plate speed between supercontinent assemblies and breakups. Although there is considerable variation in plate speeds, a linear regression of the data clearly shows that average plate speed increases with time, from about 25 deg/100 Myr at the end of the Archean to about 50 deg/100 Myr today (Fig. 3).

There is also considerable variation in plate speeds between individual cratons. For instance, Baltica–Laurentia is slow at 1600 Ma, and then very fast at 1000 and 400 Ma. Amazonia–W. Africa is slow at 1450 Ma and fast at 1300 Ma. Siberia changes from slow at 200 Ma to fast at 600 Ma, the latter of which coincides with the growth of Gondwana. North China changes from very slow at 1600 Ma to very fast at 1400 Ma, the latter age perhaps recording the last stages in assembly of Nuna. India shows a tremendous burst of speed at about 400 Ma and again between 65 and 50 Ma (van Hinsbergen et al., 2011) related, respectively, to the assembly and later breakup of Gondwana. We do not find evidence for the very fast speed at ~ 600 Ma reported by Gurnis and Torsvik (1994) using a "high latitude" model. This model is challenged by others (Pisarevsky et al., 2000, 2001; Meert and Van der Voo, 2001), and two alternative models have been proposed (e.g., Pisarevsky et al., 2008; Li et al., 2008). Although the issue is still disputed, recent publications (e.g. Levashova et al., 2013) favor a "low-latitude" model, which we use in our analysis.

4. Discussion

4.1. Plate speeds and collision rates

The most striking changes during the assemblies of Rodinia and Gondwana are increases in craton collision rates and average plate speed for Gondwana. Again, note that the peak in plate velocity at 1100 Ma may correspond to a partial breakup of Nuna, but it also corresponds to the initial collisions leading to Rodinia. As plate tectonics is the surface manifestation of mantle convection, which is driven mostly by cooling from above, plate speeds are largely controlled by slab pull forces as plates descend into the mantle. Modern plate velocities vary with the percent of plate margins that are convergent, and geodynamic modeling indicates that slab pull forces amount to about 95% of the net driving forces of plates, whereas ridge-push and drag forces at the base of the lithosphere account for no more than 5% of the total (Lithgow-Bertelloni and Richards, 1995; Conrad and Lithgow-Bertelloni, 2002). Thus, the increasing plate speeds and craton collision frequency during assemblies

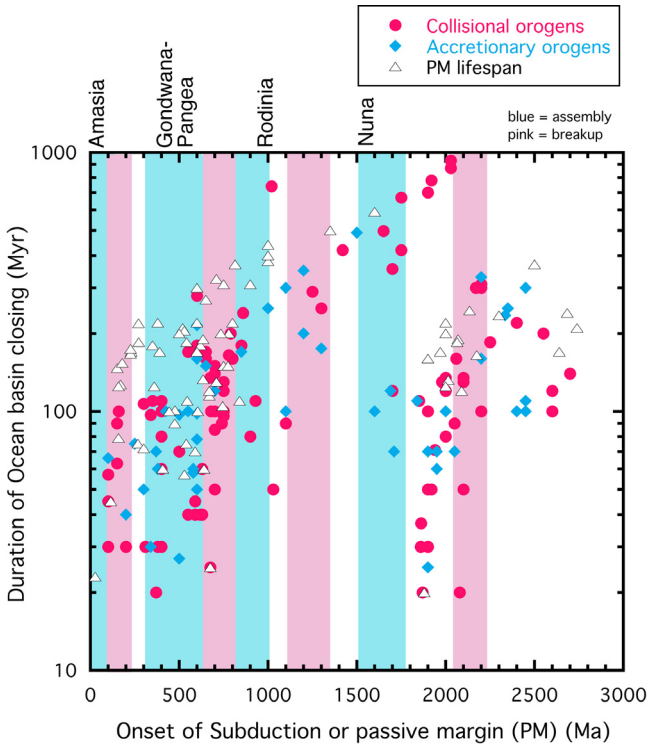

Fig. 5. Durations of ocean basin closings and passive margins from the Neoarchean onwards. Passive margins from Bradley (2008). Orogens given in Appendix 1 (Pt 1). Also shown are supercontinent assembly (blue stripes) and breakup (pink stripes) times. PM, passive margin. Other information given in Fig. 1.

of Rodinia and Gondwana–Pangea may reflect an increasing percentage and/or rate of subduction at convergent margins at these times. These observations are also consistent with the accretionary orogen model of Cawood and Buchan (2007) and Cawood et al. (2009).

Nuna, however, is different and shows remarkably low plate speeds and craton collision frequencies during assembly (Fig. 3). The peak in collision frequency at 1850 Ma and rapid fall in numbers of cratons thereafter is the consequence of collision and suturing of many small Archean cratons following fragmentation of Neoarchean supercratons. Some might regard these collisions as an early stage in the formation of Nuna; however, most of the amalgamation of Nuna occurred between 1700 and 1500 Ma when plate speeds and collision frequencies were minimal (Pisarevsky et al., 2014a,b). Unlike the breakup of Neoarchean supercratons at 2200–2100 Ma, large numbers of dispersing cratons are not seen in the paleomagnetic record after Nuna assembly. This may mean that Nuna was never fully fragmented and that large pieces survived in tact, or with only minor re-arrangements of blocks, in later supercontinents (Meert, 2013). Clearly the tectonic controls on assembly of Nuna were very different from Rodinia and Gondwana–Pangea.

4.2. Ocean basin durations

The durations of ocean basin closings fall into the same two groups as passive margins, as proposed by Bradley (2008) (Fig. 5), which is suggestive of two evolutionary cycles. The two cycles are apparent for both accretionary and collisional orogens. It should be noted, however, that ocean basin closing durations as estimated from onset of subduction (Appendix 1, Pt 1) may not be the same as passive margin durations, since passive margins begin during ocean

basin openings. Hence, onsets of subduction are only minimum values for durations of passive margins. The earliest ocean basin closing cycle begins in the Neoarchean and ends about 1900 Ma, and the younger cycle begins about 1900 Ma and extends to the present; there may be up to 100 Myr overlap between the two cycles. The younger cycle seems to begin with the onset of the supercontinent cycle. It shows decreasing durations of ocean basin closing from 2000 to 1000 Ma and afterwards duration shows no relation to age (Fig. 5). There is a faint suggestion of a similar pattern in the older cycle, but scatter in the data do not require a decrease in ocean basin closing duration with time at any point in the cycle. One criticism of Bradley's passive margin plot is that it lacks examples with short durations in the early cycle, which could be due to lack of data or poor resolution. However, with our new data, we have added examples with shorter durations ($\leq$50 Myr) to both the older and younger cycles, thus supporting the existence of two cycles as originally proposed by Bradley (2008).

All of the orogens shown in Fig. 5 for the younger cycle with onsets of subduction >1500 Ma are either long-lived accretionary orogens or collisional orogens with long-lived accretionary phases. After 1800 Ma, there is a sudden shift in ocean basin closing duration from mostly $\leq$100 Myr to $\geq$400 Myr. This shift is chiefly in response to the appearance of the Great Proterozoic Accretionary Orogen (and related accretionary orogens) along the Baltica–Laurentia side of Nuna and to a similar accretionary orogen in Amazonia (Condie, 2013) (Fig. 1). These accretionary orogens lasted for $\geq$500 Myr until the Grenvillian collisions that formed Rodinia. This leaves us with two obvious questions: (1) why don't we see similar jumps in ocean basin closing durations near the onsets of assembly of Rodinia and Gondwana–Pangea, and (2) why do ocean basin closing times decrease with age within the younger cycle prior to 1000 Ma (corresponding to durations of $\geq$200 Myr) and perhaps not at all in the older cycle?

A possible answer to first question is that except for the Altaids orogen (long-lived before collision with North China craton at 280 Ma), which shows a jump in duration, there were no long-lived ($\geq$500 Myr) accretionary orogens preceding the assemblies Rodinia and Gondwana–Pangea. Although Terra Australis began about 900 Ma (Cawood, 2005; Cawood et al., 2009; Bahlburg et al., 2009), it is still active. When it finally closes some time in the future, perhaps a new ocean-basin duration cycle will begin, displaced above the younger cycle in Fig. 5.

Two possible explanations for the second question are, (1) global plate speeds were proportional to the age of onset of ocean-basin closing before 1000 Ma (ocean basin closing durations of >200 Myr), but not afterwards, or (2) prior to 1000 Ma ocean basins were larger than afterwards and their closing times were proportional to the ages of onset of closure. Neither plate speeds nor collision frequency (Figs. 3 and 5; Appendix 1, Pt 1) support the first explanation. The long-lived accretionary orogens associated with Nuna, many of which remained active until Grenvillian collisions around 1000 Ma, yield some support for the second explanation. However, why closing times should be proportional to the ages of onset of closing is not clear.

A more difficult question is what determines whether long-lived or short-lived accretionary orogens develop during supercontinent assembly? Nuna lasted for at least 300 Myr (1500–1200 Ma; Appendix 1, Pt 4), perhaps never completely fragmented, and large pieces may have been transferred to Rodinia nearly in tact (for instance, Siberia–Laurentia, Congo–Tanzania–Sao Francisco, Australia–Antarctica) (Meert, 2013; and references therein). The accretionary orogens developed before the assembly of Nuna during collisions of the Archean microcratons, beginning about 1900 Ma.

4.3. Mantle plumes and the supercontinent cycle

Many investigators have suggested a relationship between arrival of mantle plumes at the base of the lithosphere and supercontinent breakup (Burke and Dewey, 1973; Hill, 1991; Courtillot et al., 1999). However, the role of mantle plumes in fragmenting or weakening the continental lithosphere in supercontinents is still a matter of uncertainty and debate (Anderson, 1994; Storey, 1995; Marzoli et al., 1999). The number of precise isotopic ages of large igneous provinces (LIPs) is continually growing and can be used to monitor major mantle plume events with increasing confidence (Ernst et al., 2011). Our existing database contains 444 precisely dated LIPs ranging in age from 3500 to 10 Ma and shows 18 peaks in LIP activity between 3450 and 100 Ma (Condie and Davaille, 2014). LIP events at 2200, 2100, 1450, 1380 (and 1450?), 800, 300, 200 and 100 Ma correlate with known supercontinent breakups or initial rifting of supercontinents (red arrows in Fig. 3). Likewise, minima in LIP activity at 2600, 1700–1500, 1100–900, and 600–400 Ma correlate with supercontinent assemblies. A major LIP event at 1850 Ma correlates with rapid collisions of Archean microcratons, another event at 600 Ma correlates with numerous craton collisions during the early stages of Gondwana assembly, and the 1100 Ma peak correlates with either or both the final breakup of Nuna or the onset of assembly of Rodinia (black arrows).

Our results support at least two types of mantle plume events: those associated with supercontinent breakup and those not associated with supercontinent breakup. The timing of breakup of various components of Pangea have long been known to be associated with putative plumes in the Atlantic and Indian ocean basins (Storey, 1995; Dalziel et al., 2000; Davaille et al., 2005; Li et al., 2008), although continental breakup magmatism by itself does not necessarily demand mantle plumes. Many models have been proposed for mantle plume episodicity, and among the three most common are convection at high Raleigh numbers, slab avalanches, and thermochemical instabilities at the base of the mantle (Davaille et al., 2005; Arndt and Davaille, 2013). Slab avalanches from the 660-km discontinuity depend on the Clapeyron slope of the perovskite reaction, of which recent estimates suggest the slope is too small to support avalanches, even at higher mantle temperatures (Katsura et al., 2003; Fei et al., 2004). The thermochemical instability model has the advantage that it can explain all major LIP events by one process, and it is strongly supported by experimental results. It also implies that LIP events that correspond to supercontinent assembly are independent of what is happening in the lithosphere and have deep-seated causes (Condie and Davaille, 2014).

4.4. Supercontinent Lifetimes

Some investigations have suggested that the supercontinent cycle is speeding up with time (Hoffman, 1997; Condie, 2002). Part of the problem of establishing the timing of the supercontinent cycle is related to incomplete breakup of supercontinents and to what constitutes a new supercontinent. For instance, as discussed above and also by others (Roberts, 2011), Nuna may have never completely fragmented, but large blocks survived either intact, or nearly intact to be incorporated in later supercontinents. Perhaps fragments were jostled around but no new large ocean basins appeared during Nuna fragmentation. If this is the case, Rodinia and younger supercontinents, at least in part, formed from large surviving fragments of Nuna. Pannotia presents another difficulty. Dalziel (1997) suggested that the short-lived supercontinent Pannotia (Laurentia–Baltica–Siberia and Gondwana) formed about 600 Ma then rapidly split up again (560–530 Ma) (see also Murphy and Nance, 2008; Scotese, 2009). However, there is strong evidence that Laurentia and Baltica broke apart at ca. 600 Ma with the opening of the eastern Iapetus (e.g. Bingen et al., 1998; Greiling

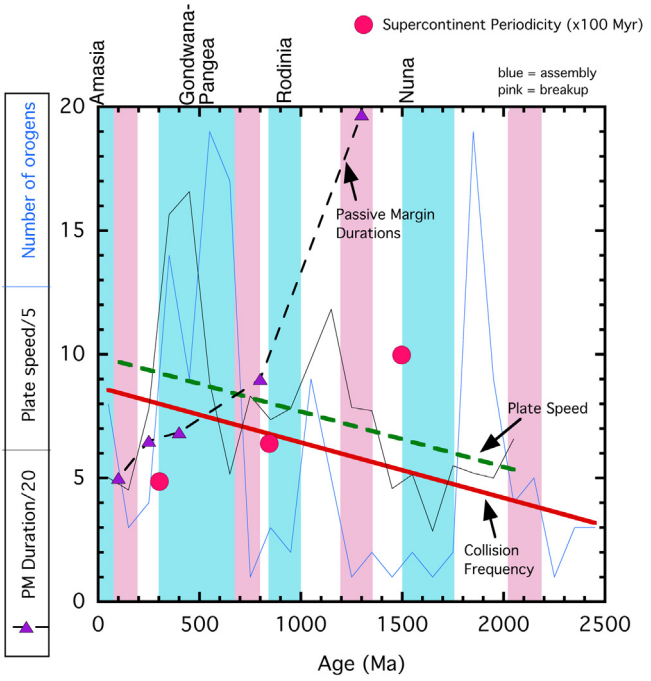

Fig. 6. Periodicity of the supercontinent cycle (from data in Appendix 1, Pt 4) compared to passive margin durations (from Bradley, 2008) and calculated plate speeds and craton collision frequency (from Fig. 3). Period is measured from the end of assembly of one supercontinent to the end of assembly of the next supercontinent.

et al., 1999; Cawood et al., 2001; Siedlecka et al., 2004; Cawood and Pisarevsky, 2006, 2008 and references therein), and that an ocean was opening between Laurentia and Siberia at the same time (Pisarevsky et al., 2014a,b). Thus, there is diminishing evidence to support the existence of Pannotia.

If we assume that Nuna fragmented, at least in part, and that Pannotia did not exist, the resulting supercontinent cycle is illustrated in Figs. 3 and 6. Nuna has a maximum lifetime of about 300 Myr (1500–1200 Ma), Rodinia 100 Myr (850–750 Ma), and Gondwana–Pangea 200 Myr (350–150 Ma) (Appendix 1, Pt 4). If Neoarchean supercratons are included as part of the supercontinent cycle, they appear to have endured for at least 300 Myr (2500–2200 Ma) and some of them for perhaps longer (Bleeker, 2003). The period of the supercontinent cycle is 650 Myr for Nuna to Rodinia and 500 Myr for Rodinia to Gondwana–Pangea (Appendix 1, Pt 4) (or up to 1000 Myr if the late Archean supercratons are included), which agrees with the results of Torsvik et al. (2002) and Zhang et al. (2009). Supercontinent assembly times are the order of 150–300 Myr, and breakup times, 100–200 Myr. Supercontinent assembly and breakup overlap at 700–600 Ma (Rodinia–Gondwana) and Amasia begins to assemble while Pangea is still breaking up at 150–100 Ma (Condie, 2002). Thus, if Gondwana is counted as part of Pangea, both average plate speeds and frequency of craton collisions suggest that the frequency of supercontinent assembly is increasing with time (Fig. 6). Our results support the geodynamic models of Phillips and Bunge (2007), which suggest that regular spacing of the supercontinent cycle is unlikely when many cratons are involved. It is also noteworthy that the history of angular plate velocities and that of passive margins, which are derived independently to each other, both suggest a gradual increase in speed of plate tectonics (Fig. 6). Although there are other supporting observations such as the cooling history of the upper mantle (Herzberg et al., 2010) and the abundance of radiogenic xenon in the atmosphere (Padhi et al., 2012), the history of angular plate velocities may be the most direct evidence for more sluggish plate tectonics in the past.

Based on the frequency of supercontinent formation summarized by Hoffman (1997), Korenaga (2006) tried to estimate the secular change of a globally averaged plate motion. Whether or not Gondwana is counted as part of Pangea is the largest uncertainty in his study as well. The formation of a supercontinent involves more than the tempo of plate tectonics, with obvious factors including the global pattern of mantle convection and the strength of suture zones. Unless we are discussing a very simple situation, such as two-plate plate tectonics (e.g., Gurnis, 1988), it may be too optimistic to seek a definitive answer to secular change in the supercontinent cycle. Focusing on individual events, such as the life span of passive margins or the history of craton collisions as herein presented, can provide more reliable measures on the overall tempo of plate tectonics through time. As shown by Bradley (2008), the lifespan of passive margins decreases significantly in the last 1500 Myr (Fig. 6). Also, supercontinent periodicity decreases from 1000 Myr (starting with the Neoarchean supercratons) to 500 Myr (Fig. 6; Appendix 1, Pt 4). These observations are inconsistent with the notion of faster plate tectonics in the past, and support the operation of more sluggish plate tectonics in the Proterozoic (Korenaga, 2003, 2006, 2013).

5. Conclusions

Major peaks in the rate of craton collision are observed at 1850 and 600 Ma with smaller peaks at 1100 and 350 Ma. Distinct minima occur at 1700–1200, 900–700, and 300–200 Ma. As expected, relatively low collision rates occur at times of supercontinent breakup (2200–2050, 1300–1200, 800–700, and 300–100 Ma). Angular plate velocities as weighted by craton area range from about 20 to 80 deg/100 Myr with two peaks at 450–350 Ma and 1100 Ma (60–80 deg/100 Myr). There is no simple relationship in craton collision frequency or average plate speed between supercontinent assemblies and breakups. Assembly of Rodinia (1000–850 Ma) and Gondwana (650–350 Ma) correlate with moderate to high rates of craton collisions and increasing plate velocities, both of which may reflect an increasing percentage of convergent margins at these times. Nuna assembly (1700–1500 Ma), however, is different and shows remarkably low plate speeds and craton collision frequencies. Clearly the tectonic controls on assembly of Nuna are very different from Rodinia and Gondwana–Pangea. The number of cratons decreases from $\geq$20 before 1900 Ma to 13–17 after this time, and is related to rapid collisions among dispersing Archean microcratons between 1900 and 1800 Ma.

Both orogens and passive margins show the same two cycles of ocean basin closing: an early cycle from Neoarchean to 1900 Ma and a later cycle from 1900 Ma to the present. The younger cycle shows decreasing durations of ocean basin closing from 1900 to 1000 Ma, and afterwards, duration shows no relation to age. The cause of these cycles is not understood, but may be related to increasing plate speeds during supercontinent assembly and whether or not long-lived accretionary orogens accompany supercontinent assembly. LIP (large igneous province) age peaks at 2200, 2100, 800, 200 and 100 Ma correlate with known supercontinent breakup, and minima in LIP activity at 2600, 1700–1500, 1100–900, and 650–400 Ma correlate with supercontinent assembly. Other LIP peaks do not correlate with the supercontinent cycle or correlate with supercontinent assemblies. A thermochemical instability model for mantle plume generation at the bottom of the mantle has the advantage that it can explain all major LIP events by one process, and it is supported by experimental results. It also implies that LIP events that correspond to supercontinent assembly are independent of what is happening in the lithosphere and have deep-seated causes.

The period of the supercontinent cycle varies from 500 to 650 Myr, or up to 1000 Myr if late Archean supercratons are included. Nuna has a duration of about 300 Myr (1500–1200 Ma), Rodinia 100 Myr (850–750 Ma), and Gondwana–Pangea 200 Myr (350–150 Ma), and breakup durations are 100–200 Myr. The history of angular plate speed, craton collision frequency, and the history of passive margins all suggest a gradual speed up of plate tectonics with time.

Acknowledgments

This is contribution 468 of the ARC Centre of Excellence for Core to Crust Fluid Systems (http://www.ccfs.mq.edu.au) and TIGeR publication 567. The paleogeographic reconstructions are made with GPLATES software (available free at www.glates.org).

Appendix.

Part 1: Characteristics of orogens (for references see Condie (2013, 2014) and Condie and Aster (2013).

	Onset subduction (Ma)	Onset deformation (Ma)	Termination deformation (Ma)	Subduction Duration (Myr)	Deformation duration (Myr)	Type (accretion acc; collision, coll)
Venezuelan	100	34	0	66	34	acc
Verkhoyansk-Kolyma	200	160	110	40	50	acc
Japan	300	250	0	50	250	acc
Indosinian	350	250	210	100	40	acc
Eastern Australia	370	300	220	70	80	acc
South America (Gondwanide)	340	310	200	30	110	acc
Antarctica	380	320	230	60	90	acc
Taimyr 2	425	325	250	100	75	acc
Antler	600	385	300	215	85	acc
Achalian (Argentina)	500	403	382	97	21	acc
Ellesmerian	600	440	360	160	80	acc
Lachlan (Tabberabberan)	550	450	410	100	40	acc
Cuyania (south Andes)	500	473	400	27	73	acc
Early Himalayan	600	502	450	98	52	acc
Ross-Delamerian	580	520	480	60	40	acc
North Andean (Famatinian)	600	522	460	78	62	acc
Pampean	580	522	460	58	62	acc
Greater Himalayan (Bimphedian)	650	500	450	150	50	acc
Saldanian (Cape belt)	600	550	510	50	40	acc
Beardmore (Antarctica)	700	580	560	120	20	acc
Lhasa terrane	850	680	660	170	20	acc
Arabian-Nubian	1000	750	680	250	70	acc
Yenisei (Siberia)	1200	850	750	350	100	acc
Kunlun	1100	1000	900	100	100	acc
Cariris Velhos (Brazil)	1200	1000	920	200	80	acc
Verkhoyansk	1500	1010	900	490	110	acc
Taimyr	1200	1000	940	200	60	acc
Eastern Ghats	1100	1085	1000	300	85	acc
Xiong'er	1300	1125	1050	175	75	acc
Danopolonian	1600	1500	1440	100	60	acc
Kararan	1690	1570	1540	120	30	acc
Olarian	1700	1580	1540	120	40	acc
Racklan-Forward	1710	1640	1600	70	40	acc
Nimrod-Ross	1840	1730	1700	110	30	acc
Tarim	1900	1830	1800	70	30	acc
Mt Isa	1900	1875	1845	25	30	acc
Lesser Himalaya	1950	1880	1780	70	100	acc
Cathaysia	1950	1890	1830	60	60	acc
Wopmay	2000	1900	1840	100	60	acc
Angara	2000	1900	1850	100	50	acc
Usagaran-Tanzania	2050	1980	1930	70	50	acc
Magondi-Kheis	2200	2040	1960	160	80	acc
Luizian	2350	2100	2000	250	100	acc
West Congo	2335	2100	2000	235	100	acc
Minas	2450	2150	2080	300	70	acc
Blezardian	2400	2300	2250	100	50	acc
Ivaro, Uruguay	2450	2340	2330	110	10	acc
Borborema (Granja)	2450	2350	2300	100	50	acc
Mineiro	2600	2450	2360	150	90	acc
Alpine	100	43	0	57	43	coll
Isparta (Turkey)	100	55	0	45	55	coll
Apulian (Italy)	150	60	0	90	60	coll
Himalayan	160	60	0	100	60	coll
Pyrenees	100	70	0	30	70	coll
Zagros (Iran)	150	87	0	63	87	coll
Brookian (Alaska)	200	170	150	30	20	coll
Karakorum (Pakistan)	300	193	150	107	43	coll
Qinling-Dabie-Sulu 4	350	240	225	110	15	coll
Kunlun, NW Tibet	340	243	230	97	13	coll
Altaids (Central Asian Orogenic Belt)	1000	280	240	720	40	col
Mixtecan, Oaxaquia	400	290	230	110	60	coll
Ouachita	400	300	230	100	70	coll
South Africa	330	300	215	30	85	coll

	Onset subduction (Ma)	Onset deformation (Ma)	Termination deformation (Ma)	Subduction Duration (Myr)	Deformation duration (Myr)	Type (accretion acc; collision, coll)
Qinling-Dabie-Sulu 3	400	320	300	80	20	coll
Tian Shan	600	320	290	280	30	coll
Uralian 2	380	350	230	30	120	coll
Variscan	370	350	270	20	80	coll
Acatecan, Oaxaquia	400	370	340	30	30	coll
Alleghanian	400	340	280	60	60	coll
Meguma (NeoAcadian)	550	380	370	170	10	coll
Qinling-Dabie-Sulu 2	500	430	420	70	10	coll
Scandian	600	420	350	180	70	coll
Acadian	600	420	390	180	30	coll
Grampian (Sotland)	650	480	437	170	43	coll
Qinling-Dabie-Sulu 1	650	490	480	160	10	coll
Taconic-Caledonian	550	510	400	40	110	coll
Damara	675	540	500	135	40	coll
Cadomian	590	545	535	45	10	coll
Dom Feliciano 2	590	550	510	40	40	coll
Pinjarra	700	550	520	150	30	coll
Zambia	700	550	520	150	30	coll
Rokelides	700	560	550	140	10	coll
Gariep (SW Kaapvaal)	630	570	543	60	27	coll
Paraguay	620	580	510	40	70	coll
Zambezi	680	580	520	100	60	coll
Malagasy	630	590	510	40	80	coll
Ribeira (SE Brazil)	790	590	510	200	80	coll
Kuungan, Antarctica	700	600	490	100	110	coll
Taimyr 1	700	600	550	100	50	coll
Timanides (Russia)	700	600	570	100	30	coll
Dahomeyide	780	615	590	165	25	coll
Oubanguides (Cameroon)	700	615	590	85	25	coll
Baikalian	750	620	550	130	70	coll
Brasilia 1	860	620	570	240	50	coll
Uralian 1	750	620	550	130	70	coll
Hoggar	750	630	580	120	50	coll
Brasilia 2	800	640	600	160	40	coll
Central African	740	650	590	90	60	coll
Dom Feliciano 1	700	650	590	50	60	coll
East African	750	650	600	100	50	coll
Mauritanides	675	650	590	25	60	coll
Anti-Atlas	750	654	545	96	109	coll
West African	850	670	650	180	20	coll
SW Tarim	900	820	780	80	40	coll
Jiangnan	930	820	750	110	70	coll
Arctic	1250	960	930	290	30	coll
Valhalla	1030	980	910	50	70	coll
Kibaran	1420	1000	950	420	50	coll
Irumides	1100	1010	950	90	60	coll
Namaqua-Natal	1300	1050	1000	250	50	coll
Makkovikian-Labradorian-Grenville	1750	1080	980	670	100	coll
Amazonia (Sunsas)	2030	1100	1000	930	100	coll
Baltica (Svecofennian-Sveconorwegian)	1920	1140	1110	780	30	coll
Shawinigan, N Blueridge province	1650	1153	1078	497	75	coll
Amazonia (Oaxaquia)	2030	1160	1080	870	80	coll
Penokean-Yavapai-Mazatzal	1900	1200	1120	700	80	coll
Albany-Fraser	1750	1330	1260	420	70	coll
Musgrave (Mt West)	1700	1345	1293	355	52	coll
Olarian	1700	1580	1540	120	40	acc
Kimban	1850	1740	1700	110	40	coll
Volyn Central Russian	1900	1800	1780	100	20	coll
Tennant	1862	1825	1800	37	25	coll
Yapungku	1860	1830	1760	30	70	coll
TransHudson	1980	1850	1800	130	50	coll
Halls Creek	1900	1850	1820	50	30	coll
Tanami	1870	1850	1830	20	20	coll
Cornian	2000	1865	1845	135	20	coll
Torngat	1940	1869	1844	71	25	coll
Aravalli	2200	1870	1850	330	20	coll
New Quebec	2170	1870	1815	300	55	coll
Nagssugtoqidian	1920	1870	1840	50	30	coll
Foxe	1900	1870	1850	30	20	coll
Ubendian	2000	1880	1850	120	30	coll
Trans-North China	2200	1890	1850	310	40	coll
Sutam (Central Aldan)	2200	1900	1850	300	50	coll
Akitkan	2060	1900	1870	160	30	coll
Lapland Granulite belt	2000	1920	1870	80	50	coll
Inglefield	2100	1950	1920	150	30	coll
Thelon	2050	1960	1910	90	50	coll
Glenburgh	2100	1965	1940	135	25	coll

	Onset subduction (Ma)	Onset deformation (Ma)	Termination deformation (Ma)	Subduction Duration (Myr)	Deformation duration (Myr)	Type (accretion acc; collision, coll)
Taltson	2100	1970	1930	130	40	coll
Volga-Don (Pachelma)	2100	2050	2000	50	50	coll
Limpopo	2080	2060	1970	20	90	coll
Tandilia	2250	2065	2020	185	45	coll
Birimian-Transamazonian	2200	2100	2050	100	50	coll
Salvador-Itabuna-Curaçá	2400	2180	2100	220	80	coll
Arrowsmith	2550	2350	2280	200	70	coll
Neto Rodrigues, Uruguay	2600	2480	2440	120	40	coll
Commonwealth Bay, Antarctica	2600	2500	2420	100	80	coll
MacQuoid, Rae Province	2700	2560	2500	140	60	coll

Part 2.

Number of orogens per 100 Myr moving window					Average plate speeds[a]		Number of cratons col/col + acc	
Plot age	Time window	Accretionary	Collisional	Total	deg/100Myr	deg/100Myr/5		
50	0–100	2	6	8	25.1	5.02	13	0.750
150	100–200	1	2	3	22.6	4.52		0.667
250	200–300	2	2	4	39	7.8	13	0.500
350	300–400	5	9	14	78.3	15.66		0.643
450	400–500	4	5	9	82.9	16.58	14	0.556
550	500–600	7	12	19	44.4	8.88		0.632
650	600–700	1	16	17	25.8	5.16	14	0.941
750	700–800	1	0	1	41.6	8.32		0.000
850	800–900	1	2	3	36.8	7.36	13	0.667
950	900–1000	0	2	2	39.1	7.82		1.000
1050	1000–1100	5	4	9	49	9.8	14	0.444
1150	1100–1200	1	4	5	59.1	11.82		0.800
1250	1200–1300	0	1	1	39.3	7.86	16	1.000
1350	1300–1400	0	2	2	38.6	7.72		1.000
1450	1400–1500	1	0	1	22.9	4.58	17	0.000
1550	1500–1600	1	1	2	25.7	5.14		0.500
1650	1600–1700	1	0	1	14.3	2.86	16	0.000
1750	1700–1800	1	1	2	27.5	5.5		0.500
1850	1800–1900	5	14	19	26	5.2	20	0.737
1950	1900–2000	3	6	9	25	5		0.667
2050	2000–2100	1	3	4	32.9	6.58	36	0.750
2150	2100–2200	3	2	5				0.400
2250	2200–2300	1	0	1			37	0.000
2350	2300–2400	2	1	3				0.333
2450	2400–2500	2	1	3			38	0.333

col, number of collisional orogens; acc, number of accretionary orogens.

[a] Cratons weghted by area in km^2.

Part 3: Euler rotation parameters (to the absolute framework) in Fig. 2.

Continent	Pole (deg N)	(deg E)	Angle (degrees)
	100 Ma		
North America	62.92	89.35	31.78
Greenland	40.62	90.06	25.2
Eurasia	31.13	64.7	15.62
Africa	18.9	−41.4	−25.35
India	10.28	4.78	−80.15
South America	72.19	42.81	27.11
North China	31.13	64.7	15.62
South China	31.13	64.7	15.62
Australia	17.5	36.4	−30.56
East Antarctica	80.82	109.52	−8.87
	200 Ma		
North America	61.66	31.34	63.2
Greenland	52.05	49.56	51.83
Eurasia	35.66	43.05	38.32
Africa	21.21	−54.62	−21.52
India	20.4	20.55	−76.8
South America	59.15	0.87	35.49
North China	68.74	58.67	−23.37
South China	−23.03	147.66	23.35
Australia	42.96	149.98	−42.41
East Antarctica	−31.87	−33.66	39.09
	300 Ma		
Laurentia	38.44	65.16	62.53
Greenland	24.14	76.99	58.65
Baltica	4.28	85.04	47.07

Continent	Pole (deg N)	(deg E)	Angle (degrees)
Gondwana	−14.26	132.38	63.23
North China	47.69	−43.89	−23.9
South China	3.13	−58.34	−58.68
Siberia	35.14	77.37	54.19
Tarim	12.37	84.8	37.98

Part 4: Characteristics of the supercontinent cycle (timing in Ma).

Assembly		Duration		Breakup		Period[a]	
2700–2500	200	2500–2200	300	2200–2100	100	2500–1500	1000
1700–1500	200	1500–1200	300	1300–1100	200	1500–850	650
1000–850	150	850–750	100	800–650	150	850–350	500
650–350	300	350–150	200	150–0	150	350–?	

[a] Period is measured from the end of assembly of one supercontinent to the end of assembly of the next supercontinent.

References

Anderson, D.L., 1982. Hotspots, polar wander, Mesozoic convection and the geoid. Nature 297, 391–393.

Anderson, D.L., 1994. Superplumes or supercontinents? Geology 22 (1), 39–42.

Arndt, N., Davaille, A., 2013. Episodic Earth evolution. Tectonophysics, http://dx.doi.org/10.1016/j.tecto.2013.07.002.

Bahlburg, H., Vervoort, J.D., Du Frame, S.A., Bock, B., Augustsson, C., Reimann, C., 2009. Timing of crust formation and recycling in accretionary orogens: insights learned from the western margin of South America. Earth-Sci. Rev. 97, 215–241.

Bingen, B., Demaiffe, D., van Breemen, O., 1998. The 616 Ma old Egersund basaltic dike swarm, S.W. Norway and Late Neoproterozoic opening of the Iapetus Ocean. J. Geol. 106, 565–574.

Bleeker, W., 2003. The late Archean record: a puzzle in ca. 35 pieces. Lithos 71, 99–134.

Bradley, D.C., 2008. Passive margins through earth history. Earth-Sci. Rev. 91, 1–26.

Burke, K., Dewey, J.F., 1973. Plume-generated triple junctions: key indicators in applying plate tectonics to old rocks. J. Geol. 81, 406–433.

Cawood, P.A., McCausland, J.A., Dunning, G.R., 2001. Opening Iapetus: constraints from the Laurentian margin in Newfoundland. Geol. Soc. Am. Bull. 113, 443–453.

Cawood, P.A., 2005. Terra Australis Orogen: Rodinia breakup and development of the Pacific and Iapetus margins of Gondwana during the Neoproterozoic and Paleozoic. Earth-Sci. Rev. 69, 249–279.

Cawood, P.A., Pisarevsky, S.A., 2006. Was Baltica right way up or upside down in the Neoproterozoic? J. Geol. Soc. Lond. 163, 753–759.

Cawood, P.A., Buchan, C., 2007. Linking accretionary orogenesis with supercontinent assembly. Earth-Sci. Rev. 82, 217–256.

Cawood, P.A., Kroner, A., Collins, W.J., Kusky, T.M., Mooney, W.D., Windley, B.F., 2009. Accretionary orogens through earth history. Geol. Soc. Lond. Spec. Publ. 318, 1–36.

Cawood, P.A., Pisarevsky, S.A., Leitch, E.C., 2011. Unraveling the New England orocline, east Gondwana accretionary margin. Tectonics 30, TC5002, http://dx.doi.org/10.1029/2011TC002864.

Collins, A.S., Pisarevsky, S.A., 2005. Amalgamating Eastern Gondwana: the evolution of the Circum-Indian orogens. Earth-Sci. Rev. 71, 229–270, http://dx.doi.org/10.1016/j.earscirev.2005.02.004.

Condie, K.C., 2002. The supercontinent cycle: are there two patterns of cyclicity? J. Afr. Earth Sci. 35, 179–183.

Condie, K.C., 2007. Accretionary orogens in space and time. Geol. Soc. Am. Mem. 200, 145–158.

Condie, K.C., 2013. Preservation and recycling of crust during accretionary and collisional phases of Proterozoic orogens: a bumpy road from Nuna to Rodinia. Geosciences 3, 240–261.

Condie, K.C., 2014. Growth of continental crust: a balance between preservation and recycling. Mineral. Mag. 78, 623–637.

Condie, K.C., Aster, R.A., 2013. Refinement of the supercontinent cycle with Hf, Nd, and Sr isotopes. Geosci. Front. 4, 667–680.

Condie, K.C., Davaille, A., 2014. Mantle plumes and the supercontinent cycle. In: Geological Association of Canada and Mineralogical Association of Canada, Annual Meetings, Fredericton, NB, Canada, May 21–23, 2014, Abstract, Session SY-7.

Conrad, C.P., Lithgow-Bertelloni, C., 2002. How mantle slabs drive plate tectonics. Science 298, 207–209.

Courtillot, V., Jaupart, C., Manighetti, I., Tapponnier, P., Besse, J., 1999. On causal links between flood basalts and continental breakup. Earth Planet. Sci. Lett. 166, 177–195.

Dalziel, I.W.D., 1997. Overview: Neoproterozoic–Paleozoic geography and tectonics: review, hypotheses and environmental speculations. Geol. Soc. Am. Bull. 109, 16–42.

Dalziel, I.W.D., Mosher, S., Gahagan, L.M., 2000. Laurentia–Kalahari collision and the assembly of Rodinia. J. Geol. 108, 499–513.

Davaille, A., Stutzmann, E., Silveira, G., Besse, J., Courtillot, V., 2005. Convective patterns under the Indo-Atlantic box. Earth Planet. Sci. Lett. 239, 233–252.

Davies, G.F., 2009. Effect of plate bending on the Urey ratio and the thermal evolution of the mantle. Earth Planet. Sci. Lett. 287, 513–518.

Ernst, R.E., Bleeker, W., 2010. Large igneous provinces (LIPs), giant dyke swarms, and mantle plumes: significance for breakup events within Canada and adjacent regions from 2.5 Ga to the present. Can. J. Earth Sci. 47, 695–739.

Ernst, E., Srivastava, R., Bleeker, W., Hamilton, M., 2011. Precambrian large igneous provinces (LIPs) and their dyke swarms: new insights from high-precision geochronology integrated with paleomagnetism and geochemistry. Precambrian Res. 183, vii–xi.

Fei, Y., Van Orman, J., van Westrenen, W., Sanloup, C., Minarik, W., Hirose, K., et al., 2004. Experimentally determined postspine transformation boundary in Mg_2SiO_4 uing MgO as an internal pressure standard and its geophysical implications:. J. Geophys. Res. 108, B02305, http://dx.doi.org/10.1029/2003JB002562.

Greiling, R.O., Jensen, S., Smith, A.G., 1999. Vendian–Cambrian subsidence of the passive margin of western Baltica – application of new stratigraphic data from the Scandinavian Caledonian margin. Nor. Geol. Tidsskr. 79, 133–144.

Gurnis, M., 1988. Large-scale mantle convection and the aggregation and dispersal of supercontinents. Nature 332, 695–699.

Gurnis, M., Torsvik, T.H., 1994. Rapid drift of large continents during the late Precambrian and Paleozoic: Paleomagnetic constraints and dynamic models. Geology 22, 1023–1026.

Herzberg, C., Condie, K., Korenaga, J., 2010. Thermal history of the Earth and its petrological expression. Earth Planet. Sci. Lett. 292, 79–88.

Hill, R.I., 1991. Starting plumes and continental breakup. Earth Planet. Sci. Lett. 104, 398–416.

Hoffman, P.F., 1997. Tectonic genealogy of North America. In: van der Pluijm, B.A., Marshak, S. (Eds.), Earth structure: an introduction to structural geology and tectonics. McGraw-Hill, pp. 459–464.

Katsura, T., Yamada, H., Shinmei, T., Kubo, A., Ono, S., Kanzaki, M., et al., 2003. Post-spinel transition in Mg_2SiO_4 determined by high P-T in situ X-ray diffractometry. Phys. Earth Planet. Inter. 136, 11-24.

Korenaga, J., 2003. Energetics of mantle convection and the fate of fossil heat. Geophys. Res. Lett. 30, 1437, http://dx.doi.org/10.1029/2002GL016179.

Korenaga, J., 2006. Archean geodynamics and the thermal evolution of Earth. Am. Geophys. Union Monogr. 164, 7–32.

Korenaga, J., 2007. Eustasy, supercontinental insulation, and the temporal variability of terrestrial heat flux. Earth Planet. Sci. Lett. 257, 350–358.

Korenaga, J., 2013. Initiation and evolution of plate tectonics on Earth: theories and observations. Annu. Rev. Earth Planet. Sci 41, 117–151.

Lawver, L.A., Grantz, A., Gahagan, L.M., 2002. Plate kinematic evolution of the present Arctic region since the Ordovician. In: Miller, E.L., Grantz, A., Klemperer, S.L. (Eds.), Tectonic Evolution of the Bering Shelf-Chukchi Sea-Arctic Margin and Adjacent Landmasses, Special Paper. Geological Society of America, Boulder, CO, pp. 333–358.

Levashova, N.M., Bazhenov, M.L., Meert, J.G., Kuzhetsov, N.B., Golovanova, I.V., Danukalov, K.N., Fedorova, N.M., 2013. Paleogeography of Baltica in the Ediacaran: Paleomagnetic and Geochronological data from the clastic Zigan Formation, South Urals. Precambrian Res. 236, 16–30.

Li, Z.X., Powell, C.McA., 2001. An outline of the palaeogeographic evolution of the Australasian region since the beginning of the Neoproterozoic. Earth-Sci. Rev. 53, 237–277.

Li, Z.X., Bogdanova, S.V., Collins, A.S., Davidson, A., De Waele, B., Ernst, R.E., Fitzsimons, I.C.W., Fuck, R.A., Gladkochub, D.P., Jacobs, J., Karlstrom, K.E., Lu, S., Natapov, L.M., Pease, V., Pisarevsky, S.A., Thrane, K., Vernikovsky, V., 2008. Assembly, configuration, and break-up history of Rodinia: a synthesis. Precambrian Res. 160, 179–210.

Lithgow-Bertelloni, Richards, M.A., 1995. Cenozoic plate driving forces. Geophys. Res. Lett. 22, 1317–1320.

Lowman, J.P., Jarvis, G.T., 1995. Mantle convection models of continental collision and breakup incorporating finite thickness plates. Phys. Earth Planet. Inter. 88, 53–68.

Marzoli, A., Renne, P.R., Piccirillo, E.M., Ernesto, M., Bellieni, G., De Min, A., 1999. Extensive 200-Million-year-old continental flood basalts of the Central Atlantic Magmatic Province. Science 284, 616–618.

McElhinny, M.W., McFadden, P.L., 2000. Paleomagnetism: Continents and Oceans. Academic Press, San Diego, 386 pp.

McElhinny, M.W., Powell, C.McA., Pisarevsky, S.A., 2003. Paleozoic terranes of Eastern Australia and the drift history of Gondwana. Tectonophysics 362, 41–65, http://dx.doi.org/10.1016/S0040-1951(02)00630-3.
Meert, J.G., Van der Voo, R., 2001. Comment on 'New palaeomagnetic result from Vendian red sediments in Cisbaikalia and the problem of the relationship of Siberia and Laurentia in the Vendian' by S. A. Pisarevsky, R. A. Komissarova and A. N. Khramov. Geophys. J. Int. 146, 867–870.
Meert, J.G., 2014. Strange attractors, spiritual interlopers and lonely wanderers: the search for pre-Pangean supercontinents. Geosci. Front. 5, 155–166.
Moores, E.M., Yikilmaz, M.B., Kellogg, L.H., 2013. Tectontics: 50 years after the revolution. Geol. Soc. Am. Spec. Pap. 500, 321–369.
Murphy, J.B., Nance, R.D., 2008. The Pangea conundrum. Geology 36, 703–706.
Nance, R.D., Murphy, J.B., 2013. Origins of the supercontinent cycle. Geosci. Front. 4, 439–448, http://dx.doi.org/10.1016/j.gsf.2012.12.007.
Nance, R.D., Murphy, J.B., Santosh, M., 2014. The supercontinent cycle: a retrospective essay. Gondwana Res. 25, 4–29.
Padhi, C., Korenaga, J., Ozima, M., 2012. Thermal evolution of Earth with xenon degassing: a self-consistent approach. Earth Planet. Sci. Lett. 341–344, 1–9.
Phillips, B.R., Bunge, H.-P., 2007. Supercontinent cycles disrupted by strong mantle plumes. Geology 35, 847–850.
Phillips, B.R., Bunge, H.-P., Schaber, K., 2009. True polar wander in mantle convection models with multiple, mobile continents. Gondwana Res. 15, 288–296.
Pesonen, L.J., Elming, S.-A., Mertanen, S., Pisarevsky, S.A., D'Agrella-Filho, M.S., Meert, J., Schmidt, P.W., Abrahamsen, N., Bylund, G., 2003. Palaeomagnetic configuration of continents during the Proterozoic. Tectonophysics 375, 289–324, http://dx.doi.org/10.1016/S0040-1951(03)00343-3.
Pisarevsky, S.A., Komissarova, R.A., Khramov, A.N., 2000. New palaeomagnetic results from Vendian red sediments in Cisbaikalia and the problem of the relationship of Siberia and Laurentia in the Vendian. Geophys. J. Int. 140, 598–610.
Pisarevsky, S.A., Komissarova, R.A., Khramov, A.N., 2001. Reply to the comment of J.G. Meert and R. Van der Voo "New palaeomagnetic results from Vendian red sediments in Cisbaikalia and the problem of the relationship of Siberia and Laurentia in the Vendian". Geophys. J. Int. 146, 871–873.
Pisarevsky, S.A., Wingate, M.T.D., Powell, C.MCA., Johnson, S., Evans, D.A.D., 2003. Models of Rodinia assembly and fragmentation. In: Yoshida, M., Windley, B., Dasgupta, S. (Eds.), Proterozoic East Gondwana: supercontinent assembly and breakup. Geol. Soc. Lond. Spec. Publ. 206, 35–55.
Pisarevsky, S.A., Murphy, J.B., Cawood, P.A., Collins, A.S., 2008. Late Neoproterozoic and Early Cambrian palaeogeography: models and problems. In: Pankhurst, R.J., Trouw, R.A.J., Brito Neves, B.B., de Wit, M.J. (Eds.), West Gondwana: Pre-Cenozoic Correlations Across the South Atlantic Region. Geol. Soc. Lond. Spec. Publ. 294, 9–31, http://dx.doi.org/10.1144/SP294.2 0305-8719/08.
Pisarevsky, S.A., Elming, S.-A., Pesonen, L.J., Li, Z.-X., 2014a. Mesoproterozoic paleogeography: supercontinent and beyond. Precambrian Res. 244, 207–225.
Pisarevsky, S.A., Wingate, M.T.D., Li, Z.X., Wang, X.C., Tohver, E., Kirkland, C.L., 2014b. Age and paleomagnetism of the 1210 Ma Gnowangerup–Fraser dyke swarm, Western Australia, and implications for late Mesoproterozoic paleogeography. Precambrian Res. 246, 1–15.
Pradhan, V.R., Pandit, M.K., Meert, J.G., 2008. A cautionary note of the age of the paleomagnetic pole obtained from the Harohalli dyke swarms, Dharwar craton, southern India. In: Srivastava, R.K., Sivaji, Ch., Chalapati Rao, N.V. (Eds.), Indian Dykes: Geochemistry, Geophysics, and Geochronology. Narosa Publishing Ltd., New Delhi, India, pp. 339–352.
Roberts, N.M.W., 2011. Increased loss of continental crust during supercontinent amalgamation. Gondwana Res. 21, 994–1000, http://dx.doi.org/10.1016/j.gr.2011.08.001.
Schubert, G., Stevenson, D., Cassen, P., 1980. Whole planet cooling and the radiogenic heat source contents of the Earth and Moon. J. Geophys. Res. 85, 2531–2538.
Siedlecka, A., Roberts, D., Nystuen, J.P., Olovyanishnikov, V.G., 2004. Northeastern and northwestern margins of Baltica in Neoproterozoic time: evidence from the Timanian and Caledonian Orogens. In: Gee, D.G., Pease, V.L. (Eds.), The Neoproterozoic Timanide Orogen of Eastern Baltica. Geol. Soc. Lond. Mem. 30, 169–190.
Scotese, C.R., 2009. Late proterozoic plate tectonics and paleogregraphy: a tale of two supercontinents, rodinia and pannotia. Geol. Soc. Lond. Spec. Publ. 326, 67–83.
Storey, B.C., 1995. The role of mantle plumes in continental breakup: case histories from Gondwanaland. Nature 377, 301–308.
Torsvik, T.H., Van der Voo, R., Meert, J.G., Mosar, J., Walderhaug, H.J., 2001. Reconstructions of the continents around the North Atlantic at about the 60th parallel. Earth Planet. Sci. Lett. 187, 55–69.
Torsvik, T.H., Van der Voo, R.V., Redfield, T.F., 2002. Relative hotspot motions versus true polar wander. Earth Planet. Sci. Lett. 202, 185–200.
Van der Voo, R., 1993. Paleomagnetism of the Atlantic, Tethys and Iapetus Oceans. Cambridge University Press, Cambridge, UK, 412 pp.
van Hinsbergen, D.J.J., Steinberger, B., Doubrovine, P.V., Gassmoller, R., 2011. Acceleration and deceleration of India-Asia convergence since the Cretaceous: rocles of mantle plumes and continental collsion. J. Geophys. Res. 116, B06101, http://dx.doi.org/10.1029/2010JB008051.
Wingate, M.T.D., Pisarevsky, S.A., De Waele, B., 2010. Paleomagnetism of the 765 Ma Luakela volcanics in northwest Zambia and implications for Neoproterozoic positions of the Congo craton. Am. J. Sci. 310, 1333–1344, http://dx.doi.org/10.2475/10.2010.05.
Worsley, T.R., Nance, R.D., Moody, J.B., 1984. Global tectonics and eustasy for the past 2 billion years. Mar. Geol. 58, 373–400.
Worsley, T.R., Nance, R.D., Moody, J.B., 1985. Proterozoic to recent tectonic tuning of biogeochemical cycles. In: Sunquist, E.T., Broecker, W.S. (Eds.), The Carbon Cycle and Atmospheric CO_2: Natural Variations Archean to Present. Am. Geophys. Union Geophys. Monogr. 32, 561–572.
Yoshida, M., Santosh, M., 2011. Supercontinents, mantle dynamics and plate tectonics: a perspective based on conceptual vs. numerical models. Earth-Sci. Rev. 105, 1–24.
Zhang, N., Zhong, S., McNarmara, A.K., 2009. Supercontinent formation from stochastic collision and mantle convection models. Gondwana Res. 15, 267–275.
Zhong, S., Zhang, N., Li, Z.-X., Roberts, J.H., 2007. Supercontinent cycles, true polar wander, and very long-wavelength mantle convection. Earth Planet. Sci. Lett. 261, 551–564.